ACADEMIA ROMÂNĂ
Revue Roumaine de Chimie
http://web.icf.ro/rrch/

Rev. Roum. Chim.,
2022, *67*(3), 207–216
DOI: 10.33224/rrch.2022.67.3.09

ELECTROCHEMICAL BEHAVIOR OF URIC ACID AT A GLASSY CARBON ELECTRODE MODIFIED WITH POLY-NINHYDRIN DERIVATIVE

Chunxiao HE,* Lijie HOU and Yan WANG

College of Chemistry and Chemical Engineering, Longdong University, Qingyang, 745000, People's Republic of China

Received January 29, 2022

Glassy carbon electrode (GCE) modified with poly-ninhydrin derivative (poly-ninhydrin derivative/GCE) was prepared by electrodeposition. The electrochemical behavior of uric acid (UA) at the modified electrode was investigated by using cyclic voltammetry. It was found that the reaction of UA on this electrode was controlled by diffusion, and the calibration curve was obtained from 5.0×10^{-5} to 3.0×10^{-3} mol/L with the detection limit of 6.4×10^{-7} mol/L. Due to the electrostatic attraction between sulfonate ions and UA cations, the electrochemical signal of UA at poly-ninhydrin derivative/GCE improved significantly compared with GCE and poly-ninhydrin/GCE. Using chronocoulometry technique, the transfer number of electrons during the heterogeneous reaction was estimated as 2. Also, the interference experiments displayed that UA could be selectively determined in the presence of dopamine (DA) and ascorbic acid (AA) and the peak potentials were *E* (AA) = 0.083 V, *E* (DA) = 0.307 V, *E* (UA) = 0.420 V, respectively. For the sake of testing the practical application of the electrode, the content of UA in human urine was determined and the recoveries were between 91.7% and 109.7%.

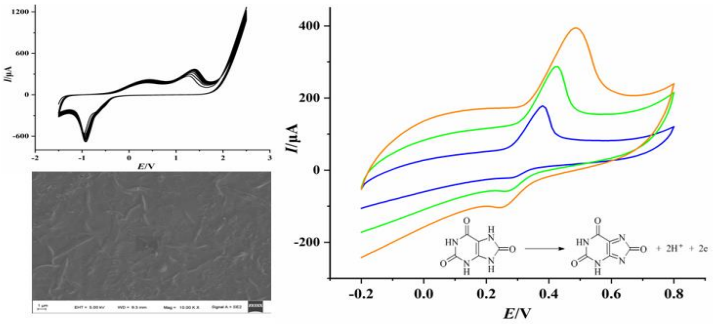

INTRODUCTION

UA is the end product of purine metabolism in human body and mainly exists in blood and urine.[1,2] According to the reports in literature, the content of UA in serum and urine of healthy adults are 0.24 ~ 0.52 mmol/L and 1.49 ~ 4.46 mmol/L respectively.[3-6] The excessive or low levels of UA in human body can lead to a variety of diseases. On the one hand, excessive concentration of UA in the body can easily form crystals and accumulate in soft tissues. It may cause several important illnesses such as gout, renal failure, congenital hyperuricemia and cardiovascular diseases. On the other hand, low level of UA in the body has enormous damage to neurons.[7-10] Therefore, the quantitative analysis of UA in human body fluid is of great significance in drug control and clinical diagnosis.

At present, the methods for detecting UA include high performance liquid chromatography, capillary electrophoresis, fluorescence method, electrochemical method, spectrophotometry and enzyme method.[11-15] Among them, electrochemical analysis are favored by the researchers due to the advantages of high accuracy, good sensitivity, wide measurement range, simple equipment, low cost and convenient automation.[16-19] In recent years, various types of modified electrodes have been used to determine the concentration of UA. Conducting

* Corresponding author: chunxiaohe211@163.com; Tel: 18152282565

polymers[20-21] have been reported as one of the promising materials for the detection of UA. Hassan *et al.*[22] synthesized poly (1,2-diaminoanthraquinone) modified electrode by adopting a continuous cyclic voltammetry technique and nickel (II) nanoparticle ions were embedded in the polymer to accomplish the continuous determination of AA, DA and UA. Hathoot *et al.*[23] fabricated hybrid nickel hexacyanoferrate/poly (1, 5-diaminonaphthalene) modified electrode. The electrode had good catalytic properties toward the electrooxidation of AA, DA and UA, and exhibited high selectivity.

In this work, ninhydrin and sulfamic acid were used as raw materials and the poly-ninhydrin derivative modified electrode was prepared by electrodeposition method. The selectivity of the electrode was noticeably improved due to the interaction of functional groups introduced on the surface of the electrode, and the determination of UA was achieved with this electrode. It opened new ways for the determination of UA in practical samples, and the results were satisfactory.

EXPERIMENTAL

Reagents and apparatus

Electrochemical experiments were performed on RST electrochemical workstation, which purchased from Zhengzhou Shi Rui Si Instrument Technology Co., Ltd. Scanning electron microscopy (SEM) was performed using a Model ULTRA Plus system (Carl Zeiss AG, Ltd., Germany). The pH value was measured by pHS-3C acidity meter. Ultrasonic cleaner was used to clean working electrodes. Electrochemical measurements were achieved based on a conventional three-electrode cell. Bare and modified glassy carbon electrodes (GCE) with diameter of 2.0 mm were used as the working electrodes. Platinum sheet and saturated calomel electrode (SCE) were used as the auxiliary electrode and reference electrode, respectively.

UA was purchased from Shanghai Aladdin Biochemical Technology Co., Ltd. Phosphate buffer solution (PBS) was obtained from stock solutions of Na_2HPO_4 and NaH_2PO_4. All the reagents used in the experiment were of analytical grade without further purified. Double distilled water was empolyed throughout in all measurements. All the experiments were carried out at room temperature.

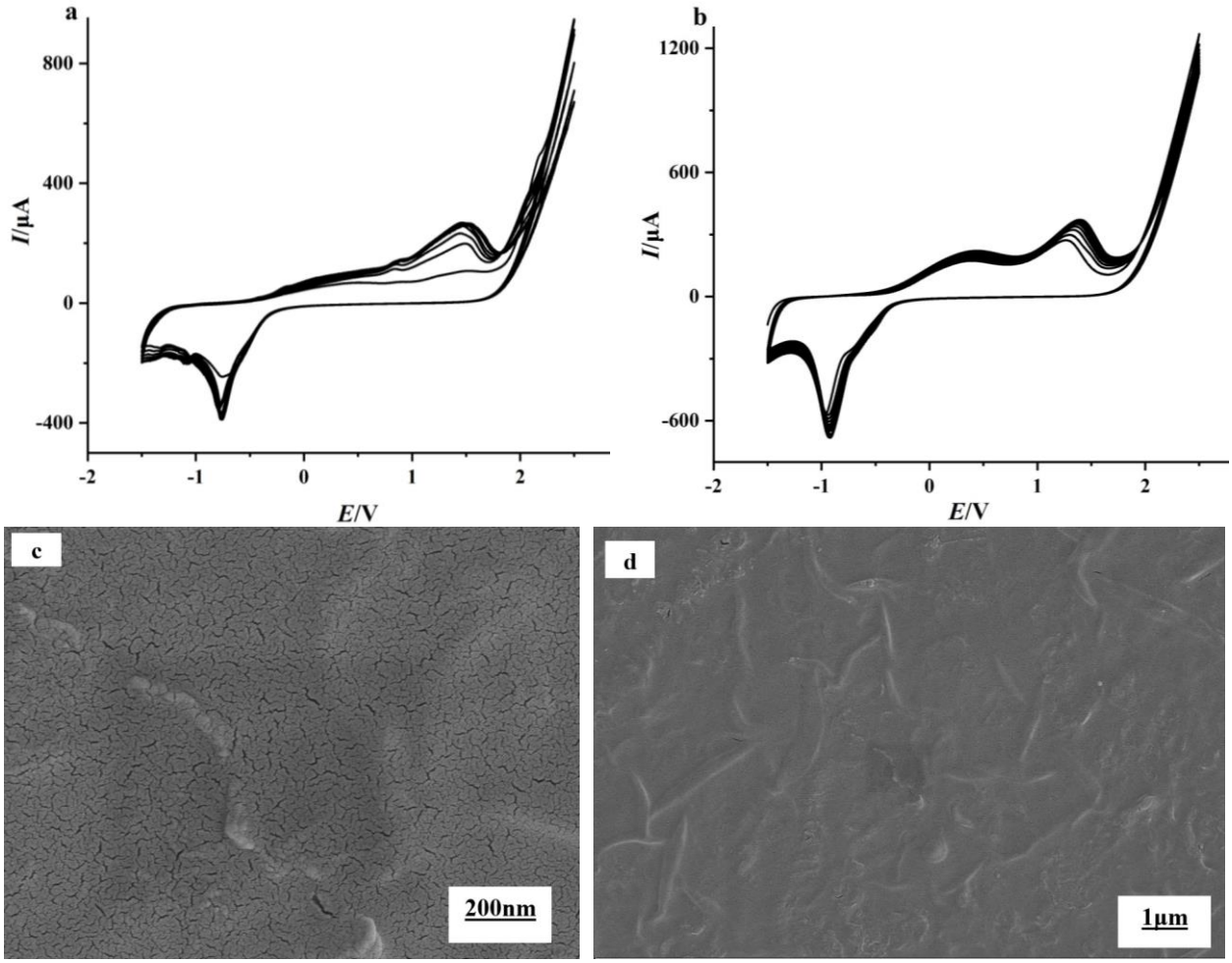

Fig. 1 – (a) Cyclic voltammogram of ninhydrin deposited on the surface of GCE, (b) Cyclic voltammogram of sulfamic acid on poly-ninhydrin/GCE, SEM images of high (c) and Low (d) magnifications of poly-ninhydrin derivative composite.

Preparation of modified electrode

Before modification, the GCE was polished mechanically with 0.3 μm and 0.05 μm alumina powder in turn, then cleaned successively with nitric acid (1:1) and anhydrous ethanol by mans of ultrasonic cleaner for 2 min, and finally rinsed with double distilled water again for later use.

The poly-ninhydrin/GCE was obtained by cyclic voltammetry for 8 cycles at a scanning rate of 0.05 V/s with cycling from -1.5 V to 2.5 V in 1mmol/L ninhydrin solution and the cyclic voltammogram of ninhydrin deposited on the surface of GCE was shown in Fig. 1(a). Can be seen from the diagram, there were a pair of larger oxidation and reduction peaks formed at 1.4 V and -0.8 V. At the same time, two smaller reduction peaks were observed at -1.1 V and -1.4 V, which were the polymerization peaks of ninhydrin molecules. With the increase of scanning rate, the current gradually increased, but the increment tapered off and the deposition rate slowed down, which proved that the polymer film deposited on the surface of the electrode was becoming saturated with polymerization. The current retained constant when scanning for 8 cycles, displaying that the amount of electropolymerization reached maximum.

The ninhydrin polymer modified on the electrode was electrochemically treated in 2 mmol/L sulfamic acid solution. Figure 1 (b) was the cyclic voltammogram of sulfamic acid on poly-ninhydrin modified electrode by scanning for 13 cycles with the same sweep rate and potential range as before. The purpose of electrochemical retreatment is to introduce sulfonate ions onto the surface of the electrode by the reaction of polymer of ninhydrin with sulfamic acid, so the modified electrode is called poly-ninhydrin derivative/GCE. According to the experimental phenomenon, the reaction mechanism is deduced as follows:

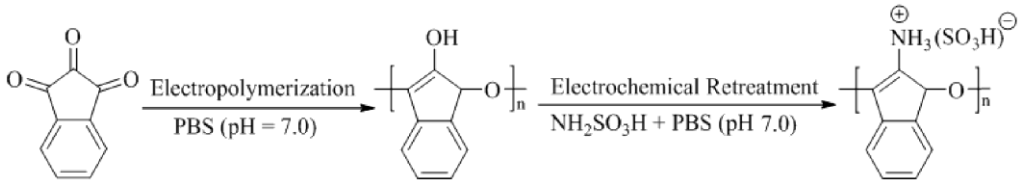

The morphological characterization of GCE modified with poly-ninhydrin derivative composite was investigated by SEM. As shown in Fig. 1(c-d), an uneven and corrugated accumulation structure with nanoscale cracks was observed. This phenomenon revealed that the modified layer was grown on the GCE substrate.

Analytical procedure

Unless otherwise noted, poly-ninhydrin derivative/GCE was used as working electrode. 0.25 mol/L PBS (pH 7.0) was used as supporting electrolyte added in 1.0×10^{-3} mol/L UA in the process of measurement. The cyclic voltammograms were recorded at a scanning rate of 0.1 V/s in the potential range of -0.2 ~ 0.8 V for UA.

RESULT AND DISCUSSION

Effect of supporting electrolyte

The experiment revealed that different types of buffer solution for UA not only affected the peak current and peak potential, but also affected the shape of the peak obviously. Therefore, the electrochemical behavior of UA in PBS (1), KH_2PO_4-NaOH (2), phthalic acid-HCl (3) and HAc-NaAc (4) buffer solution was investigated, and the results were presented in Fig. 2 (a). As can be seen from the figure, the peak currents were very small and the peak potentials were about 0.6 V in phthalic acid-HCl and HAc-NaAc buffer solutions. Meanwhile, the shape of the peak was poor in both of these solutions. However, the peak potential of UA decreased about 0.2 V in PBS and KH_2PO_4-NaOH buffer solution, the oxidation peak was well-shaped and the peak current increased significantly. Considering the value of the peak current, PBS was selected as the supporting electrolyte in the experiment.

The effect of the concentration of PBS on the peak current of UA was studied in Fig.2 (b). It could be found that the peak current increased firstly and then decreased with the increase of the concentration of PBS and obtained maximum value when the concentration of PBS reached 0.25 mol/L, so the optimal concentration of PBS was chosen as 0.25 mol/L.

Effect of buffer solution pH

In order to explore the appropriate pH value of PBS and the mechanism of electrode reaction for UA, the influence of pH value within the limits of 5.5 ~ 8.0 on peak current was researched and the results were displayed in Fig.3. Figure 3 (a) was the cyclic voltammogram of UA at different pH values and Figure 3 (b) revealed the effect of pH value on peak current of UA. It was found that the value of peak potential gradually reduced throughout during the process of increasing pH value, while the peak current increased until the pH value reached 7.0 and then decreased. Therefore, we had chosen 7.0 as the optimum pH value of PBS.

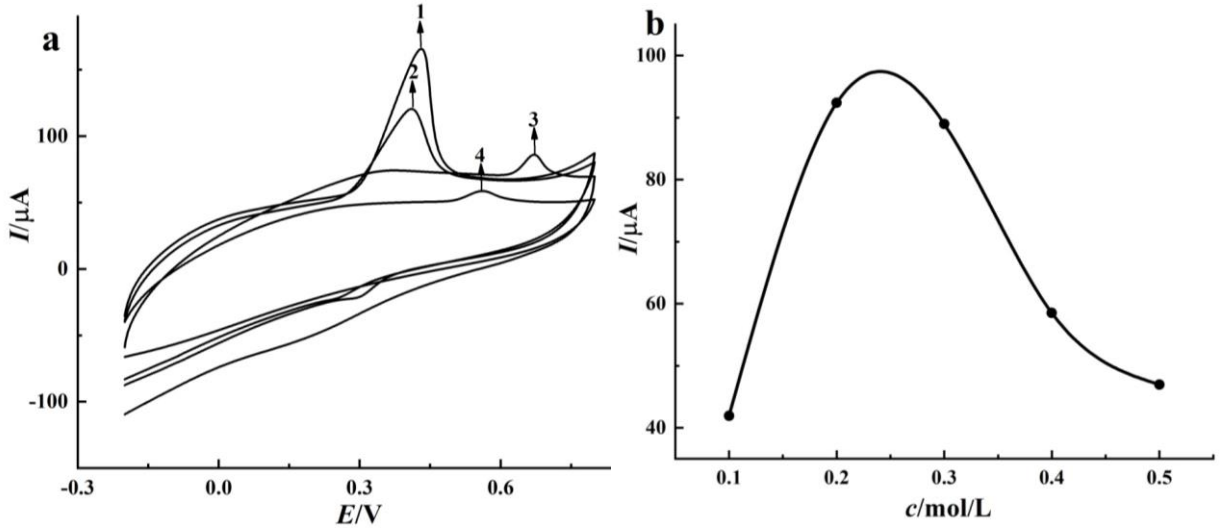

Fig. 2 – (a) Cyclic voltammogram of UA in different buffer solutions: (1) PBS, (2) KH_2PO_4- NaOH, (3) phthalic acid- HCl, (4) HAc-NaAc, (b) the effect of PBS concentration on peak current.

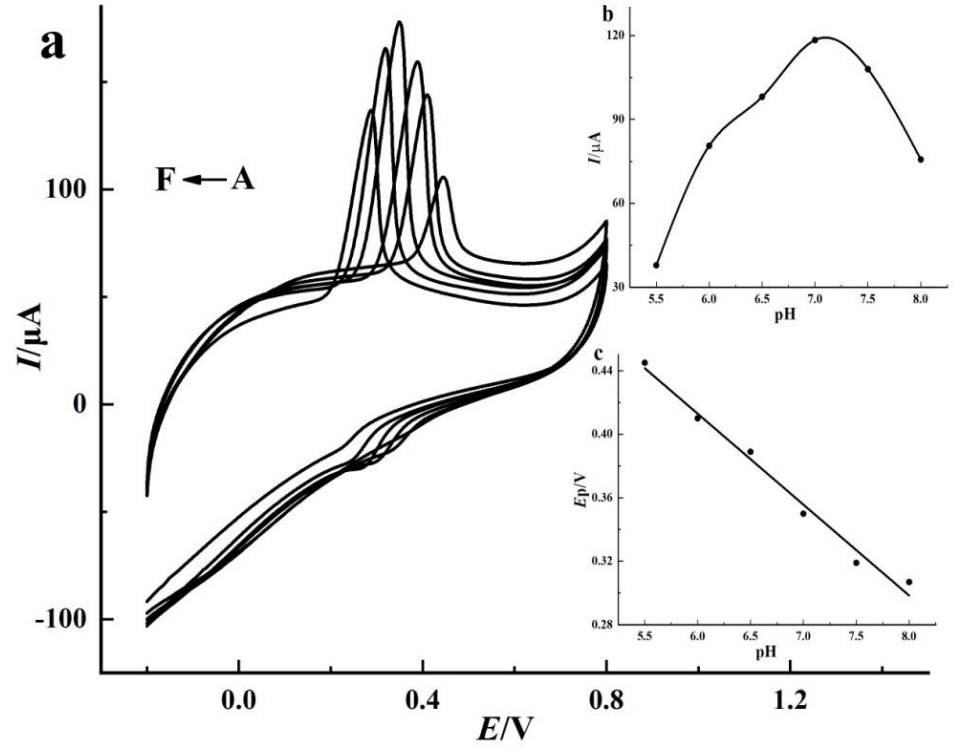

Fig. 3 – (a) Cyclic voltammogram of UA at different pH values: (A) 5.5, (B) 6.0, (C) 6.5, (D) 7.0, (E) 7.5, (F) 8.0, (b) the effect of pH value on peak current of UA, (c) the relationship between the peak potential and pH value.

The effect of the pH value on the peak potential was presented in Fig. 3 (c). It revealed that *E*p was good linearly related to pH value within the range from 5.5 to 8.0. The linear equation was *E*p = -0.0573pH + 0.7565 (*R* = 0.9927). According to the Nernst equation[24], d*E*p/dpH = -2.303*mRT*/*nF*, where *m* is the number of protons, *n* is the number of electrons involved in the reaction, *R*, *T*, *F* are the gas constant, absolute temperature, Faraday constant, respectively. It can conclude that the slope of the line which constructed by plotting Ep versus pH is -0.059 V/pH if *m*=*n*, and the slope will deviate -0.059 V/pH if *m*≠*n*. From the slope of the equation, *m*/*n* is calculated as 0.97, which is close to 1(*m*=*n*) and the experimental error is in the acceptable scope, indicating that the number of protons and electrons involved in the redox reaction of UA at poly-ninhydrin derivative/GCE are same.

Electrochemical behavior of UA at different electrodes

Cyclic voltammograms of UA at GCE (a), poly-ninhydrin/GCE (b) and poly-ninhydrin derivative/ GCE (c) were obtained in PBS (pH 7.0) and displayed in Fig. 4. It can be clearly observed that the peak current of UA at the modified electrode increased obviously in comparison to the bare electrode (I = 99 μA) and reached the maximum at the poly-ninhydrin derivative/GCE, I = 199 μA, which was about twice as high as that of the bare electrode. The results showed that a large number of negatively charged sulfonate ions were introduced on the surface of composite membrane modified electrode, which could adsorb UA cations by electrostatic attraction and enhanced the electrochemical signal of UA.[25] Owing to the reason above, poly-ninhydrin derivative/GCE had good catalytic performance toward UA.

Effect of scan rate

To further explore the reaction mechanism of UA at poly-ninhydrin derivative/GCE, the influence of the scan rate on peak current was investigated by cyclic voltammetry under different scan rates from 0.1 to 0.8 V/s with an interval of 0.05 V/s. The results were shown in Fig. 5. As can be seen from the figure, the peak current increased gradually with the increase of scan rate. In the range of 0.1 ~ 0.8 V/s, the peak current was proportional to the square root of scan rate, and the linear equation was $I = 368.07v^{1/2} + 16.07$ ($R^2 = 0.9903$), indicating that the reaction rate was controlled by the diffusion of UA[26].

Chronocoulometry

For the diffusion-controlled process, chrono-coulometry could be used to determine the transfer number of electrons during the heterogeneous reaction at the poly-ninhydrin derivative/ GCE. Chronocoulometric curves in PBS containing (a) 1.0×10^{-3} mol/L UA and (b) 0 mol/L UA (the blank for a) were shown in Fig.6. Inset curve was the linear relationship between the charge Q (μC) minus the background charge of blank solution (Q_{dl}) and the square root of time ($t^{1/2}$). As may be seen from the diagram, the quantity of electric charge (Q-Q_{dl}) exhibited excellently linear with $t^{1/2}$. For the linear equation, the slope was 23.785 μC/s$^{1/2}$ and correlation coefficient (R) was 0.9981.

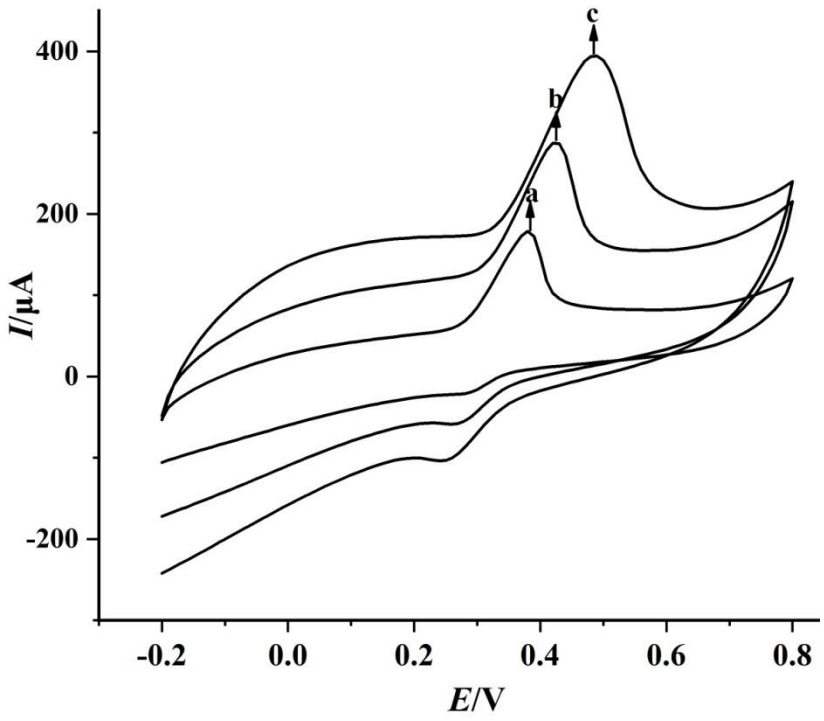

Fig. 4 – Cyclic voltammogram of UA at different electrodes:
(a) GCE, (b) poly-ninhydrin/GCE, (c) poly-ninhydrin derivative/GCE.

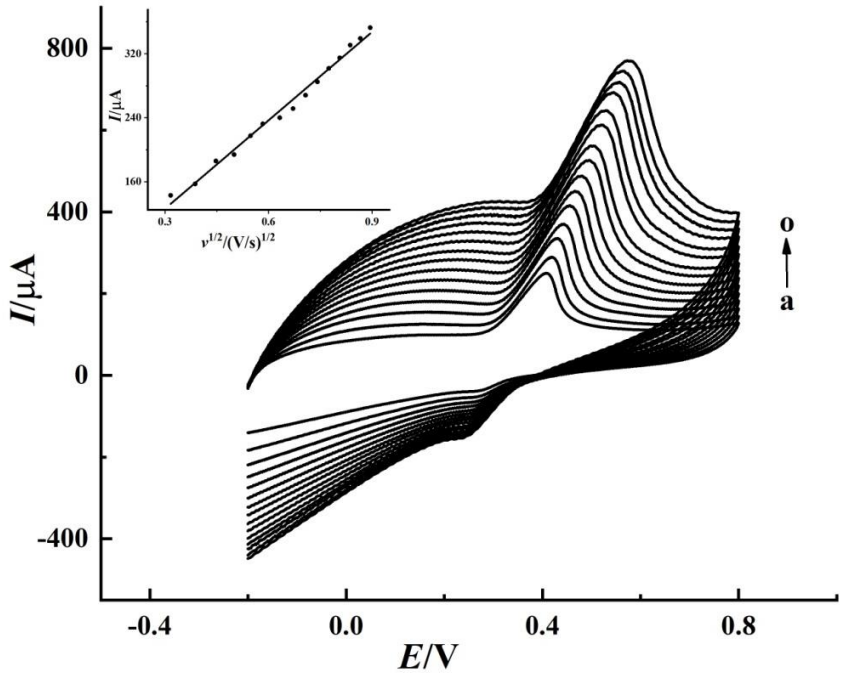

Fig. 5 – Cyclic voltammogram of UA at different scan rates: (a) 0.1, (b) 0.15, (c) 0.2, (d) 0.25, (e) 0.3, (f)0.35, (g) 0.4, (h) 0.45, (i) 0.5, (j) 0.55, (k) 0.6, (l) 0.65, (m) 0.7, (n) 0.75, (o) 0.8. Inset curve shows the relationship between the peak current and the square root of scan rate.

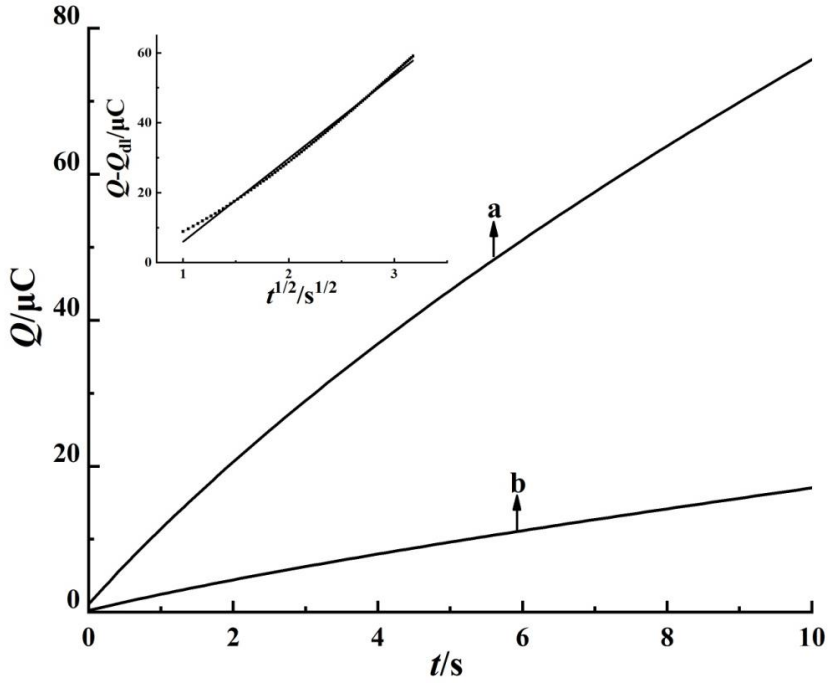

Fig. 6 – Chronocoulometric curves of UA solution (a) and blank solution (b). Inset curve shows the relationship between the charge Q (μC) minus the background charge of blank solution (Q_{dl}) and the square root of time.

According to the Cottrell equation:[1,27] $Q = 2nFAD^{1/2}c\pi^{-1/2}\ t^{1/2} + Q_{dl}$, where n is the number of electrons, F is the Faraday constant (F = 96500 C/mol), A is the surface area of the electrode (A = 0.0314 cm^2), c is the concentration of UA ($c = 1\times 10^{-3}$ mol/L), D is the diffusion coefficient ($D = 8.66 \times 10^{-6}$ cm^2/s). On the basis of the slop of (Q- Q_{dl}) *vs* $t^{1/2}$, the value of n is calculated as 2.36. That is, n = 2. Based on the results of previous experiments, we can conclude that the number of electrons and protons involved in the reaction of UA at the poly-ninhydrin derivative/GCE were 2. The results are consistent with those reported in literature.[15,27,28] Therefore, the reaction mechanism can be inferred as follows:

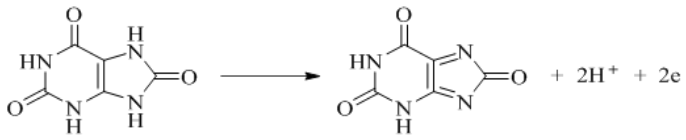

Calibration plot

Figure 7 showed the cyclic voltammograms of UA under different concentrations at the poly-ninhydrin derivative/GCE. The inset curve proved that the peak current was linear to the concentration of UA in the range from 5.0×10^{-5} to 3.0×10^{-3} mol/L. The linear equation was I=0.1505c + 4.1867 (R^2=0.9968), and the detection limit for UA was 6.4×10^{-7} mol/L. The results suggested that there was a wide linear range for determination of UA by using this electrochemical sensor.

Furthermore, the analytical performance of the proposed sensor was compared with other sensors reported in the literature for detection of UA and the results were listed in Table 1. As is shown in the table, the sensor exhibited satisfactory performance in terms of linear range and detection limit.

Stability and reproducibility

Stability and reproducibility are important indicators which decide whether the proposed sensor can be practically used in analytical application. Under the optimal conditions, the stability of the poly-ninhydrin derivative/GCE was investigated for measuring the peak current of UA every 1 hour. As shown in Fig. 8, the peak current basically remained unchanged within 5 hours, with the standard deviation of 4.8%.

The reproducibility of the sensor was obtained by successive measurements of UA for 15 times with the standard deviation of 3.2%. The results indicated that the sensor showed a good response toward UA and could be used for the determination of UA.

Interference experiment

According to literature reports,[36-38] AA and DA often coexist with UA in cellular fluids. They are functional biomolecules which involve in several physiological processes. Since these three substances have similar peak potentials on the conventional electrodes, it faces considerable challenge to determine them separately without any modifications. Therefore, poly-ninhydrin derivative/GCE was used for selective determination of UA in the presence of AA and DA in this work.

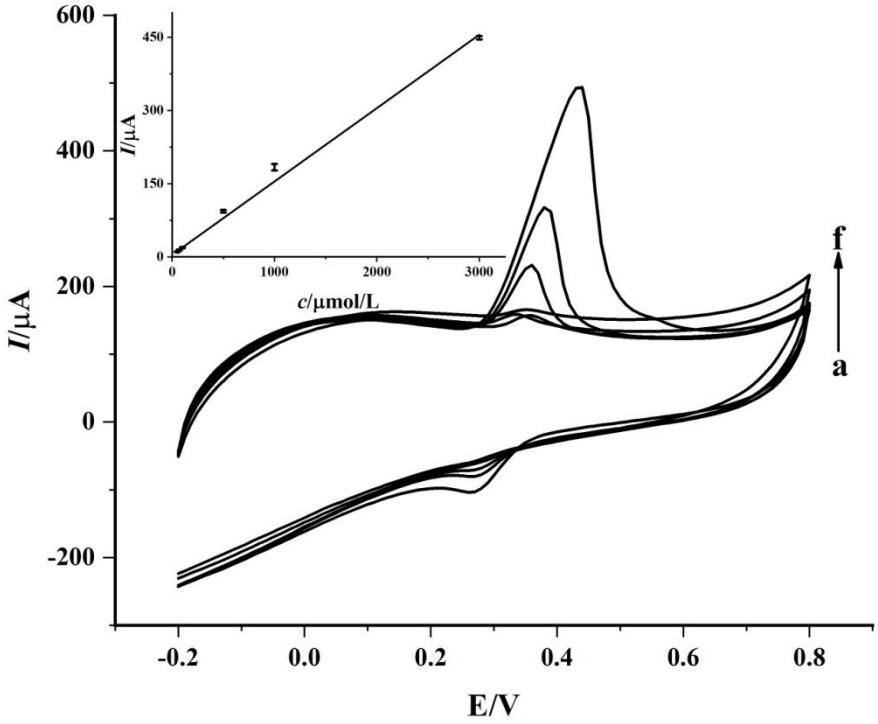

Fig. 7 – Cyclic voltammograms for different concentration of UA (from a to f: 50, 70, 100, 500, 1000, 3000 μmol/L). Inset curve shows the relationship between the peak current and the concentration of UA.

Table 1

Comparison of analytical performance of proposed sensor with other sensors for the determination of UA

Electrodes	Electrochemical technique	Linearity (μM)	Detection limit (μM)	Reference
Ur/CuO/ZnO/ITO/glass bioelectrode	CV	50~1000	5.45	[29]
EBNBHCNPE	DPV	20~700	15	[30]
Ni/PDAAQ@GC ME	SWV	100~1000	1.2	[22]
CeO_{2-x}/C/rGO/GCE	Amperometry	49.8 ~ 1050	2.0	[31]
GO/$TmPO_4$/GCE	DPV	10~100	3.73	[16]
MoS_2/PEDOT/GCE	DPV	2~25	0.95	[32]
mp-GR/GCE	DPV	5~120	2.0	[33]
GNP/Ch/GCE	DPV	1.2~100	1.6	[34]
HNP-AuAg/GCE	DPV	5.0~425	1.0	[35]
Au/CNT-PCA/GCE	Chronoamperometry	1.0~240	1.0	[28]
PCA/Au	DPV	60~700	5	[14]
PCN/MWCNT/GCE	DPV	0.2~20	0.139	[17]
poly-ninhydrin derivative/GCE	CV	50~3000	0.64	This work

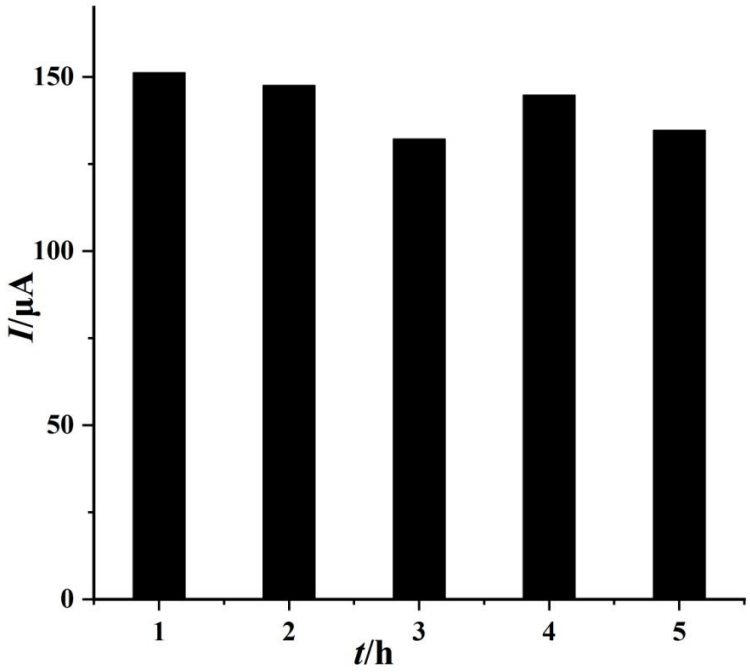

Fig. 8 – The effect of the storage time on the peak current of UA.

Figure 9 explored the electrochemical behavior of AA, DA and UA at the modified electrode. Curve a, b and c represented the cyclic voltammograms of AA, DA and UA at different concentrations. As can be seen from the figure, these three substances were obviously separated, and the peak potentials were *E* (AA) = 0.083 V, *E* (DA) = 0.307 V, *E* (UA) = 0.420 V, respectively, indicating that the sensor had good selectivity and could eliminate the interference of AA and DA.

Analytical application

The practical application of the proposed sensor was evaluated by determining the content of UA in urine samples from healthy adult male. During the measurement, all the samples were diluted with PBS and the concentration of UA was measured by standard addition method. The results were listed in Table 2. It can be found that the concentration of UA in the diluted urine was 162.9 μmol/L. Thus

the content of UA in the original urine was calculated as 4.072 mmol/L, which was consistent with the normal level of UA in the urine of healthy adults (1.49 mmol/L ~ 4.46 mmol/L). The recoveries for the spiked samples were between 91.7% and 109.7%, indicating that the method was reliable and accurate for determination of UA.

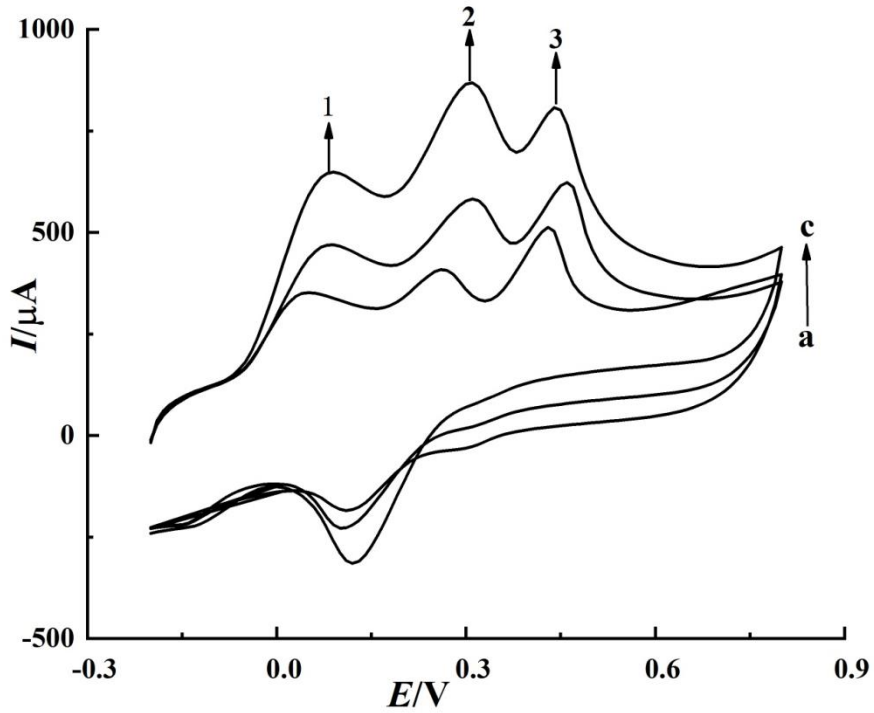

Fig. 9 – Cyclic voltammograms of AA (1), DA (2) and UA (3) at poly-ninhydrin derivative/GCE: (a) 1.0×10^{-2} mol·L^{-1} AA + 1.0×10^{-3} mol·L^{-1} DA + 1.0×10^{-3} mol·L^{-1} UA (b) 2.0×10^{-2} mol·L^{-1} AA + 2.0×10^{-3} mol·L^{-1} DA +2.0×10^{-3} mol·L^{-1} UA (c) 3.0×10^{-2} mol·L^{-1} AA + 3.0×10^{-3} mol·L^{-1} DA + 3.0×10^{-3} mol·L^{-1} UA.

Table 2

The content of UA in urine samples

Urine sample	Specified (μmol·L^{-1})	Added (μmol·L^{-1})	Theoretical content (μmol·L^{-1})	Found (μmol·L^{-1})	Recovery (%)
1	162.9	50	212.9	217.7	109.7
2		75	237.9	231.7	91.7
3		100	262.9	261.5	98.7

CONCLUSION

The electrochemical behavior of UA at poly-ninhydrin derivative/GCE was studied by using cyclic voltammetry. The results demonstrated that the modified electrode showed excellent electrocatalytic activities towards the oxidation of UA, which was mainly ascribed to the electrostatic attraction between sulfonate ions and UA cations. Also, it exhibited the superior anti-interference ability towards the oxidation of UA in the presence of AA and DA. Furthermore, the proposed sensor showed attractive performance with wide linear range, low detection limit, excellent stability as well as good reproducibility. Most importantly, the developed methodology was successfully applied to the determination of UA in human urine with satisfactory results. Therefore, the newly developed sensor should have a good application potential for electrochemical detection of UA in the future.

Acknowledgments. This work is supported by the Science and Technology Plan Project of Qingyang (No. QY2021B-F001), the Innovation Foundation Project of Gansu Education Department (No. 2021B-275) and the Youth Foundation Project of Gansu Science and Technology Department (No. 21JR7RM193).

REFERENCES

1. M. Amiri-Aref, J. B. Raoof and R. Ojani, *Ionics*, **2016**, *22*, 125-134.
2. H. Beitollahi, J. B. Raoof, H. Karimi-Maleh and R. Hosseinzadeh, *J. Solid State Electrochem.*, **2012**, *16*, 1701-1707.
3. N. B. Li, L. M. Niu and H. Q. Luo, *Microchim. Acta*, **2006**, *153*, 37-44.
4. L. Fu, Y. Zheng, A. Wang, W. Cai, B. Deng and Z. Zhang, *Arab. J. Sci. Eng.*, **2016**, *41*, 135-141.
5. S. M. Ghoreishi, M. Behpour and M. H. M. Fard, *J. Solid State Electrochem.*, **2012**, *16*, 179-189.
6. M. Noroozifar, M. Khorasani-Motlagh, M. B. Parizi and R. Akbari, *Ionics*, **2013**, *19*, 1317-1327.
7. Z. Bai, N. Gao, H. Xu, X. Wang, L. Tan, H. Pang and H. Ma, *Microchim. Acta*, **2020**, *187*, 483-494.
8. G. A. Tığ, G. Günendi and S. Pekyardımc, *J. Appl. Electrochem.*, **2017**, *47*, 607-618.
9. M. Asif, H. Sajid, K. Ayub, M. A. Gilani, M. S. Akhter and T. Mahmood, *J. Mol. Model.*, **2021**, *27*, 244-254.
10. K. M. Hassan and M. A. Azzem, *J. Appl. Electrochem.*, **2015**, *45*, 567-575.
11. D. Huang, Y. Cheng, H. Xu, H. Zhang, L. Sheng, H. Xu, Z. Liu, H. Wu and S. Fan, *J. Solid State Electrochem.*, **2015**, *19*, 435-443.
12. A. Manbohi and S. H. Ahmadi, *Chem. Pap.*, **2020**, *74*, 2675-2687.
13. M. Mazloum-Ardakani, A. Naser-Sadrabadi, M. A. Sheikh-Mohseni, A. Benvidi, H. Naeimi and A. Karshenas, *Ionics*, **2013**, *19*, 1663-1671.
14. L. M. Niu, N. B. Li and W. J. Kang, *Microchim. Acta*, **2007**, *159*, 57-63.
15. X. Pang, F. Li, S. Huang, Z. Yang, Q. Mo, L. Huang, W. Xu, L. Chen and X. Li, *Anal. Bioanal. Chem.*, **2020**, *412*, 669-680.
16. H. Huang, Y. Yue, Z. Chen, Y. Chen, S. Wu, J. Liao, S. Liu and H. Wen, *Microchim. Acta*, **2019**, *186*, 189-197.
17. J. Lv, C. Li, S. Feng, S. Chen, Y. Ding, C. Chen, Q. Hao, T. Yang and W. Le, *Ionics*, **2019**, *25*, 4437-4445.
18. M. Mazloum-Ardakani, M. A. Sheikh-Mohseni, H. Beitollahi, A. Benvidi and H. Naeimi, *Turk. J. Chem.*, **2011**, *35*, 573-585.
19. Z. Hsine, S. Blili, R. Milka, H. Dorizon, A. H. Said and H. Korri-Youssoufi, *Anal. Bioanal. Chem.*, **2020**, *412*, 4433-4446.
20. M. P. Massafera and S. I. C. De-Torresi, *Electroanalysis*, **2011**, *23*, 2534-2540.
21. S. Mahalakshmi and V. Sridevi, *Electrocatalysis*, **2021**, *12*, 415-435.
22. K. M. Hassan, *J. Iran. Chem. Soc.*, **2018**, *15*, 1007-1014.
23. A. A. Hathoot, K. M. Hassan, W. A. Essa and M. Abdel-Azzem, *J. Iran. Chem. Soc.*, **2017**, *14*, 1789-1799.
24. L. Zhang, C. Liu, Q. Wang, X. Wang and S. Wang, *Microchim. Acta*, **2020**, *187*, 149-158.
25. L. Zhang, Z. Shi and Q. Lang, *J. Solid State Electrochem.*, **2011**, *15*, 801-809.
26. Y. Shi, J. Wang, S. Li, B. Yan, H. Xu, K. Zhang and Y. Du, *Nanoscale Res. Lett.*, **2017**, *12*, 455-461.
27. Y. Wang, *Microchim. Acta*, **2011**, *172*, 419-424.
28. B. Posha, H. Kuttoth and N. Sandhyarani, *Microchim. Acta*, **2019**, *186*, 672-682.
29. K. Jindal, M. Tomar and V. Gupta, *Sensor. Actuat. B*, **2017**, *253*, 566-575.
30. H. Beitollahi, M. M. Ardakani, H. Naeimi and B. Ganjipour, *J. Solid State Electrochem.*, **2009**, *13*, 353-363.
31. B. Peng, J. Cui, Y. Wang, J. Liu, H. Zheng, L. Jin, X. Zhang, Y. Zhang and Y. Wu, *Nanoscale*, **2018**, *10*, 1939-1945.
32. Y. Li, H. Lin, H. Peng, R. Qi and C. Luo, *Microchim. Acta*, **2016**, *183*, 2517-2523.
33. X. Zhu, Y. Liang, X. Zuo, R. Hu, X. Xiao and J. Nan, *Electrochim. Acta*, **2014**, *143*, 366-373.
34. P. Wang, Y. Li, X. Huang and L. Wang, *Talanta*, **2007**, *73*, 431-437.
35. J. Hou, C. Xu, D. Zhao and J. Zhou, *Sensor. Actuat. B Chem.*, **2016**, *225*, 241-248.
36. M. Asif, A. Aziz, H. Wang, Z. Wang, W. Wang, M. Ajmal, F. Xiao, X. Chen and H. Liu, *Microchim. Acta*, **2019**, *186*, 61-71.
37. T. K. Aparna and R. Sivasubramanian, *J. Chem. Sci.*, **2018**, *130*, 14-24.
38. Y. Wu, P. Deng, Y. Tian, J. Feng, J. Xiao, J. Li, J. Liu, G. Li and Q. He, *J. Nanobiotechnol.*, **2020**, *18*, 112-124.